ChemComm

β-Peptide Bundles: Design. Build. Analyze. Biosynthesize.

Journal:	*ChemComm*
Manuscript ID	CC-FEA-02-2016-001546.R1
Article Type:	Feature Article
Date Submitted by the Author:	19-Apr-2016
Complete List of Authors:	Wang, Pam; Yale University, Department of Chemistry Schepartz, Alanna; Yale University, Department of Chemistry

ChemComm

FEATURE ARTICLE

β-Peptide Bundles: Design. Build. Analyze. Biosynthesize.

Pam S. P. Wang[a] and Alanna Schepartz[a,b]

Received 00th January 20xx,
Accepted 00th January 20xx

DOI: 10.1039/x0xx00000x

www.rsc.org/chemcomm

Peptides containing β-amino acids are unique non-natural polymers known to assemble into protein-like tertiary and qauternary structures. When composed solely of β-amino acids, the structures formed, defined assemblies of 14-helices called β-peptide bundles, fold cooperatively in water solvent into unique and discrete quaternary assemblies that are highly thermostable, bind complex substrates and metal ion cofactors, and, in certain cases, catalyze chemical reactions. In this Perspective, we recount the design and elaboration of β-peptide bundles and provide an outlook on recent, unexpected discoveries that could influence research on β-peptides and β-peptide bundles (and β-amino acid-containing proteins) for decades to come.

Introduction

It has been almost a century since Svedberg reported that polypeptides prepared from α-amino acids could assemble into discrete, multi-subunit quaternary structures.[1] The formation of discrete quaternary structures enables diversity and specificity at the molecular level and has guided the evolution of cellular processes that are believed essential for the development of life from simple precursors.[2] Moreover, the discovery that functional control can be afforded *via* the regulation of protein quaternary structure has accelerated the development of nanoscale devices with broad applications in science and engineering.[3-8] For many years it was believed that natural biopolymers—specifically, polypeptides composed of α-amino acid monomers, RNA, and DNA—were unique in their ability to assemble in water into unique, cooperatively folded molecular entities. In this Perspective, we recount the design and elaboration of β-peptide bundles, which lack even a single α-amino acid, yet fold cooperatively into thermostable entities that embody many protein-like functions.

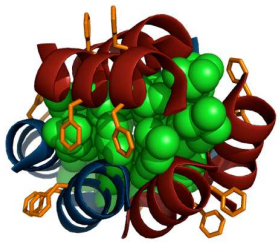

Figure 1. The first β-peptide bundle Zwit-1F: a defined array of eight identical β-peptide monomers.

[a] Department of Chemistry, Yale University, 225 Prospect St. New Haven CT 06511
[b] Department of Molecular, Cellular, and Developmental Biology, New Haven CT 06511.

† Footnotes relating to the title and/or authors should appear here.
Electronic Supplementary Information (ESI) available: [details of any supplementary information available should be included here]. See DOI: 10.1039/x0xx00000x

Foldamers[9] are non-α-peptide oligomers that can fold into well-defined secondary structures.[7] Examples include β-peptides,[10] γ-peptides,[11] δ-peptides,[12] peptoids,[13] azapeptides,[14] oligoureas,[15] mixtures thereof, and many others. β^3-peptides have been particularly well studied, in large part because of the ease with which they are synthesized and their ability to capture the full spectrum of protein structure, from helices, sheets, and hairpins to unique quaternary folds.[16] Indeed, with this minimally expanded backbone, β^3-peptides effectively access sectors of three-dimensional space that are unavailable to natural peptides. The ability of β^3-peptides to adopt alternate structures such as the 14- and 12-helix makes these molecules especially attractive as scaffolds for engineering bioorthogonal function.

In 2007, our group at Yale reported the first high-resolution structure of a β^3-peptide quaternary fold that exhibited protein-like properties.[17] This structure—the Zwit-1F β-peptide bundle—consists of eight identical β^3-peptides, each folded into a 14-helix, arranged as a pair of tetra-helix "hands" that are cupped at a 90° angle relative to each other (Figure 1). Subsequent work demonstrated that Zwit-1F and related β-peptide bundles display kinetic and thermodynamic properties that are virtually indistinguishable from natural proteins.[18] More recent studies showcased their functional versatility, highlighting the ability to bind carbohydrate and metal ion ligands and catalyse simple chemical reactions. This review will provide a historical and personal perspective on how β-peptide bundles were designed, improved, manipulated, and ultimately endowed with function. The Perspective will conclude by recounting recent, unexpected discoveries that could influence research on β-peptides and β-peptide bundles for decades to come.

β-Peptide bundles: Taming aggregation via design

Although our lab was fortunate to solve the first high-resolution structure of a β-peptide assembly,[17] several other groups had

previously documented the ability of β-peptides to self-associate in interesting and diverse ways. The very first example of a non-covalent β-peptide assembly—a cyclic β□□peptide nanotube that functioned as a artificial transmembrane ion channel, no less—was reported by Ghadiri in 1998.[19] Several years later, Gellman reported the first hint of a helical bundled structure, albeit heterogeneous, in an assembly formed from a *trans*-2-aminocyclohexanecarboxylic acid (ACHC) and β^3-homolysine (β^3K)-rich sequence, deca-β-peptide **1** (Figure 2a).[20] Building on this finding, in 2002 DeGrado described BHBox, a β-peptide with a diverse but prescribed sequence that folded as a dimer when stabilized by an intra-dimer disulphide bond (Figure 2b). Notably, as in classic α-peptide coiled coil examples,[21-23] the disulphide dimer exhibited greater helicity (in this case, 14-helicity) than the monomer, suggesting a cooperatively folded hydrophobic interface.[24]

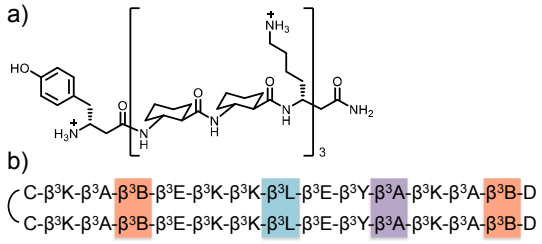

Figure 2. (a) Chemical structure of deca-β-peptide **1**, a β-peptide reported by Gellman[20] that assembles into small soluble aggregates in aqueous solution. (b) Sequence of BHBox, a disulfide-linked β-peptide dimer reported by DeGrado[24] that folds cooperatively. One-letter codes denote standard L-amino acid side-chains, except for B and D, which stand for (*S*)-3-aminovaleric acid and D-aspartic acid, respectively. Aliphatic pairs at the hydrophobic interaction interface are indicated in orange, cyan, and purple.

Design and characterization of β-peptide bundle prototypes

Our initial foray into the design of a β-peptide quaternary structure was inspired by the work of Gellman and DeGrado described above but also by that of O'Shea and Kim, whose classic studies helped define the details of coiled coil assembly and specificity in basic region leucine zipper proteins such as Fos/Jun.[25] The project at Yale was initiated by graduate student Jade Qiu: the general idea was to design a matched pair of β^3-homoleucine (β^3L)-rich β-peptides that possessed only limited 14-helix secondary structure as monomers, and exploit paired salt bridge interactions—à la Fos/Jun—to simultaneously favour hetero-oligomerization and decrease non-specific aggregation. The molecules Jade designed, Acid-1F and Base-1F (Figure 3) contained three sequence elements to achieve these goals, each localized to one 14-helix face: a quartet of β^3L residues to favour hydrophobic interactions between the monomers; a second quartet of alternating β^3-homoornithine (β^3O) and β^3-homoaspartate (β^3D) residues to improve 14-helix stability in water;[26, 27] and a set of either β^3-homoglutamate (in Acid-1F) or β^3-homoornithine (in Base-1F) to drive hetero-oligomer formation (Figure 3b).

It is fair to say that we fully expected a mixture of Acid-1F and Base-1F to assemble into a discrete coiled coil-like dimer with a 1:1 ratio of Acid-1F to Base-1F. Indeed, circular dichroism (CD) spectroscopy revealed that only a 1:1 mixture of Acid-1F and Base-1F showed a high level of 14-helix structure in dilute solution, and that the structure formed was highly stable, with a cooperative melting temperature of T_m = 58°C at 25 μM total peptide concentration. But the assembly was unquestionably not a dimer – subsequent data obtained using CD and sedimentation equilibrium analytical ultracentrifugation (SE-AU) revealed a defined assembly containing 8 β-peptide monomers, not 2.[28] Postdoctoral fellows Doug Daniels and James Petersson then joined the project, and set forth with a single goal—a high-resolution structure.

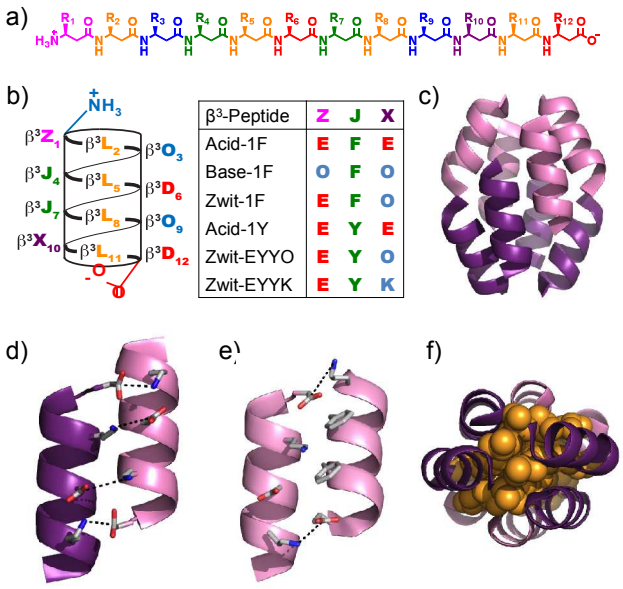

Figure 3. (a) Generic chemical structure of a β-dodecapeptide. (b) Helical net representation of a β-dodecapeptide folded into a 14-helix secondary structure and highlighting how the fold presents side chains on three well-defined helical faces. (c) Ribbon representation of the first β-peptide bundle, the homo-octamer Zwit-1F. In this representation, pairs of parallel 14-helices are shown in purple and pink that are in turn arranged in antiparallel arrays. (d-e) Close-up view of salt-bridging interactions at the (d) anti-parallel and (e) parallel helical interfaces of Zwit-1F. (f) Space-filling model (orange) showing tight packing of β^3-homoleucine side-chains in the Zwit-1F core.

The ability of Acid-1F and Base-1F to form a hetero-octamer in solution inspired Petersson to design the β-peptide Zwit-1F (Figure 3b). Like Acid-1F and Base-1F, Zwit-1F uses residues on each of the three 14-helical faces to control higher order structure. While Acid-1F and Base-1F bear cross-complementary charges at positions 1 and 10 on the third face to drive hetero-oligomerization, Zwit-1F employs self-complementary charges to favour homo-oligomerization. The incorporation of self-complementary charges into a single helix favoured the assembly of a homo-oligomeric species whose thermostability (T_m = 57°C at 50 μM) matched that of the mixed Acid-1F/Base-1F bundle. Perhaps because of this stability, it was relatively easy to obtain high quality crystals for high-resolution structural analysis. Although these crystals resisted labelling with traditional heavy metal reagents, inclusion of a single iodide at the *para* position of one pendant phenylalanine residue allowed Daniels to solve the structure at high resolution (Figure 3c). This structure confirmed the octameric stoichiometry suggested by the CD and SE-AU experiments, and revealed the unique quaternary β-peptide bundle fold, complete with a β-homoleucine (β^3L)-rich core, parallel and anti-parallel helices, and an extensive network of

interhelical electrostatic interactions (Figure 3d and 3e). The four β^3L side-chains on each β-peptide monomer are highly sequestered at the center of the bundle core, burying a total surface area of over 2000 Å^2 (Figure 3f).[17, 18]

Subsequent studies performed by Petersson using a genuine armamentarium of biophysical tools revealed that despite the absence of even a single α-amino acid, the biophysical properties of the Zwit-1F octamer are remarkably similar to those of naturally occurring α-helical bundle proteins.[18] CD and SE-AU experiments revealed that Zwit-1F self-assembles with ln K_a = 71, and a free energy of association per unit of buried surface area ΔG_{area} = 5.9 cal•mol^{-1}•Å^2. These parameters compare favorably with those of the octameric protein hemerythrin (ln K_a = 84; ΔG_{area} = 3.3 cal•mol^{-1}•Å^2), despite the much smaller size of Zwit-1F (13.1 *vs.* 110 kDa). Furthermore, as assessed by NMR H/D exchange experiments, the amide N-H of Zwit-1F at 1.5 mM concentration exchanges slowly (k_{ex} = 0.6 × 10^{-4} s^{-1}), with a rate constant corresponding to a protection factor ($P = k_{rc}/k_{ex}$, where k_{rc} is the rate constant for exchange of a random coil amide N-H) of 2 × 10^4; this protection factor slightly exceeds the value of 1 × 10^4 found for the classical GCN4 leucine zipper at 1 mM concentration.[18] The observed thermodynamic and kinetic stability of Zwit-1F rendered it an ideal prototype for the design and functionalization of a new series of protein-like β-peptide bundles.

Enhancing β-peptide bundle stability by optimizing helical interfaces

Graduate student Jessica Goodman then joined the project, and carried out a series of experiments to understand how and to what extent each design element contributed to β-peptide bundle stability. Her work led to the unexpected discovery of a new design element that has proven exceptionally useful ever since—a favoured hydrogen bonding interaction at the surface, embodied in the β-peptide bundle Acid-1Y. At the primary sequence level, Acid-1Y differs from Zwit-1F at only three positions: it contains β^3-homotyrosine (β^3Y) residues in place of β^3F residues at positions 4 and 7 and a β^3E residue in place of β^3O at position 10 (Figure 3b). While the overall ionic character of Acid-1Y deviates significantly from that of Zwit-1F (net charge of -2 vs. 0 at pH 7, respectively), the two peptides assemble into octameric bundles whose three-dimensional structures are nearly identical (RMSD = 2.0 Å) (Figure 4a). Given that the β^3F-containing peptide Acid-1F does not homo-oligomerize, the ability of Acid-1Y to self-assemble was at first surprising; however, detailed examination of its crystal structure reveals distinctive interactions between tyrosyl and aspartyl side-chains at helical interfaces (Figure 4b). Although the distances between these side-chains (average 4.1 Å) are longer than typical hydrogen bonds (1.5–2.5 Å), solvent density in the Acid-1Y crystal structure supports the presence of an extensive hydrogen-bonding network in which the tyrosyl and aspartyl side-chains participate. In terms of thermodynamic stability, Acid-1Y (T_m = 78°C at 100 μM; ln K_a = 83) further exceeds Zwit-1F (T_m = 70°C at 100 μM; ln K_a = 71), while the amide N-H protection factor for Acid-1Y (P = 6.5 × 10^4 at 750 μM) is a magnitude higher than that for Zwit-1F (P = 6 × 10^3 at 750 μM), suggesting that Acid-1Y is also kinetically more robust. In addition, the small molecule 1-anilino-8-naphthalenesulfonate (ANS)—whose fluorescence increases upon binding to hydrophobic surfaces—exhibited only a 1.6-fold increase in fluorescence in the presence of 400 μM Acid-1Y, providing evidence for its minimally exposed hydrophobic core.[29]

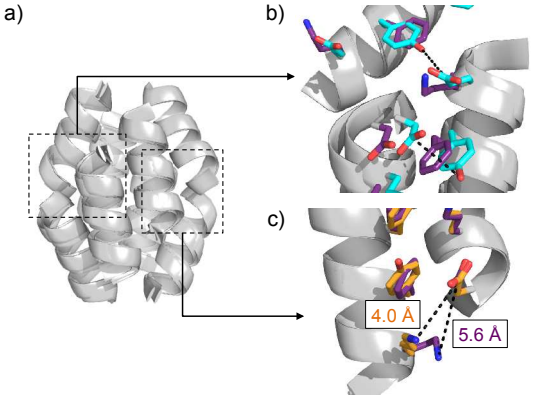

Figure 4. (a) Overlay of the Zwit-1F, Acid-1Y, and Zwit-EYYK crystal structures, showing all helical backbones in gray for simplicity. (b) Structural alignment of Acid-1Y (cyan) and Zwit-1F (purple). Dotted lines between β^3Y and β^3D side-chains indicate potential for forming H-bonding network. (c) Structural alignment of Zwit-EYYK (orange) and Zwit-1F (purple), highlighting the shorter distance between β^3K_{10} and β^3D_{12} (4.0 Å) in Zwit-EYYK compared to between β^3O_{10} and β^3D_{12} (5.6 Å) in Zwit-1F.

Graduate student Cody Craig then demonstrated that β-peptide bundle stability could be further enhanced by optimizing inter-helical salt-bridging interactions. He noticed that crystal structure of Zwit-1F shows 4 pairs of charge-complementary residues separated by distances longer than that observed typically for salt bridges in natural proteins (5.6–5.8 Å vs. 2.5–5.0 Å). Specifically, these pairs of residues occur at helical interfaces, and consist of a β^3O at position 10 of one helix and a β^3D at position 12 of an adjacent, parallel helix. Cody reasoned that substituting β^3O_{10} for a β^3-homolysine (β^3K) residue would shorten the inter-helical salt bridge by extending the basic side-chain by one methylene unit. To test this hypothesis, two derivatives of Zwit-1F—Zwit-EYYO and Zwit-EYYK—were synthesized and characterized.[30] Zwit-EYYO and Zwit-EYYK differ from Zwit-1F in the composition of their aromatic faces: both analogs contain β^3Y in place of β^3F at positions 4 and 7, with Zwit-EYYK bearing an additional β^3O to β^3K modification at position 10 (Figure 3b). Zwit-EYYK (T_m = 86°C at 50 μM; ln K_a = 94) is more thermostable than either Zwit-EYYO or Zwit-1F (T_m = 84°C and 57°C at 50 μM; ln K_a = 87 and 71, respectively), highlighting the effect of the β^3O to β^3K single residue change. The van't Hoff enthalpies for these three bundles (ΔH_{vH} = 147, 152, and 164 for Zwit-1F, Zwit-EYYO, and Zwit-EYYK, respectively) further suggest that the replacement of β^3O by β^3K contributes more to the cooperativity of unfolding than does the replacement of β^3F by β^3Y. Consistent with previous trends, the improved thermodynamic parameters of Zwit-EYYK is accompanied by greater kinetic stability; the amide N-H protection factor for Zwit-EYYK (P = 2.3 × 10^4 at 500 μM) is four times higher than that for Zwit-1F (P = 6 × 10^3 at 500 μM). Structurally, while the 14-helical backbones of Zwit-EYYK and Zwit-1F align almost perfectly (Figure 4a), the interhelical salt bridge distance in Zwit-

EYYK (4.0 Å between β^3K_{10} and β^3D_{12}) is significantly shorter than in Zwit-1F (5.6 Å between β^3O_{10} and β^3D_{12}) (Figure 4c).[30]

Progress toward a single chain β-peptide bundle

Another strategy for increasing β-peptide bundle thermodynamic stability was inspired by the properties of BHBox described above (Figure 2b),[24] in which a disulphide bond was used to favour formation of a helical dimeric assembly from a β-peptide that possessed only nascent 14-helicity as a monomer. Rather than using a disulphide bond, we sought to assemble a covalent dimer, an extended β-peptide, in which two octamer-forming Zwit-1F helices were joined through a β-homoglycine-rich linker. This approach was complicated by the relative orientation of the helix strands in the Zwit-1F octamer, in which most strands are arranged in a parallel array, not the antiparallel array required by the tandem dimer envisioned. Recognizing a unique feature of the 14-helix geometry, in which the side chain protrudes from the helix axis at an angle close to 90 degrees (the corresponding angle for an α-helix is 77.7 degrees) Petersson hypothesized that the N-C direction of one member of the parallel helical pair could be reversed and still retain the requisite interfacial packing. To test this hypothesis, we synthesized a single (albeit long!) linear β-peptide containing two Zwit-1F sequences, one of which was flipped by 180 degrees (Figure 5a). The resultant 28-residue β-peptide, Z28, was tetrameric as determined by CD and SE-AU experiments, effectively recapitulating the quaternary fold of Zwit-1F with only four subunits (Figure 5b). Z28 exhibited far greater thermodynamic stability than Zwit-1F, with T_m = 92°C at 31.25 μM. As the first example of a β-peptide that genuinely embodies all classical levels of three-dimensional structure (primary, secondary, tertiary, and quaternary) in biological macromolecules, Z28 marked an important step toward the design of larger, more protein-like β-peptides ("β-proteins").[31]

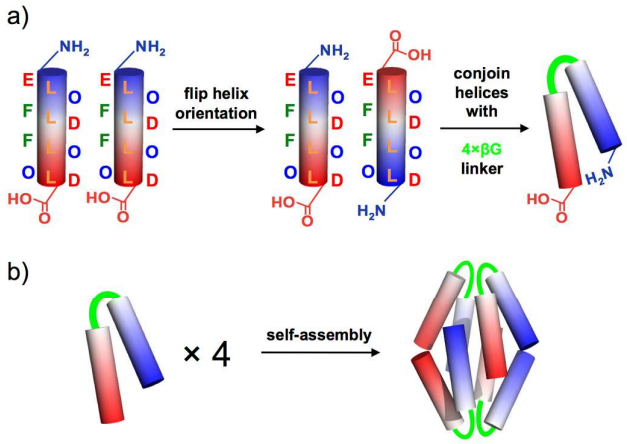

Figure 5. The design of Z28. (a) Strategy used to convert a pair of parallel Zwit-1F monomers into a single peptide chain, Z28. N- and C-termini are indicated in blue and red coloring, respectively. (b) Assembly of Z28 into a tetrameric bundle, showing a likely arrangement of helical chains that preserves the original fold of the Zwit-1F octamer.

Exploring alternate cores

It is well known that the precise identity of side chains located at the interface of natural coiled coil proteins impacts both bundle stability but bundle stoichiometry.[32] Hypothesizing that this generalization would also hold for β-peptide bundles, Jessica Goodman discovered that substituting the four β^3L side-chains in each Zwit-1F or Acid-1Y monomer for β^3V or β^3I side-chains resulted in the assembly of highly stable β-peptide tetramers;[33] this fundamental change in bundle stoichiometry echoes the conversion of the dimeric GCN4 leucine zipper into three- and four-helix bundles upon replacement of certain core leucine residues with valine or isoleucine. Compared to the parent Zwit-1F and Acid-1Y peptides, the valine derivatives Zwit-VY and Acid-VY (Figure 6a) exhibit similar thermodynamic properties, with slightly lower association constants (ln K_a = 38 and 37, respectively) and higher thermal unfolding temperatures (for Zwit-VY, T_m = 85°C at 50 μM; for Acid-VY, T_m = 85°C at 80 μM). The switch from an octameric to a tetrameric stoichiometry was originally attributed to the size difference between valine and leucine – in order for Zwit-VY and Acid-VY to maintain a tightly packed hydrophobic core, a reduction in bundle size was necessary to compensate for the loss of four methylene groups per peptide chain. In light of this hypothesis, the observation by Pam Wang that Acid-3Y—the isoleucine variant of Acid-1Y in which all four β^3L residues were replaced with β^3I (Figure 6a)—assembles into a tetramer[34] was initially surprising: Leucine and isoleucine possess the same molecular weight, with near-identical van der Waals surface areas and hydrophobic indices. The difference in stoichiometry between the isomeric β-peptides Acid-3Y and Acid-1Y suggests that their oligomeric states are controlled by the γ-carbon branching, rather than the volume, of side-chains in the hydrophobic core (Figure 6b). Interestingly, another designed β-peptide bundle comprising an all β^3V face assembles into a hexamer.[35] Natural α-peptide bundles exhibit a similar relationship between side-chain branching and stoichiometry – for example, dimeric coiled coils favor β-branched amino acids at position *a* and unbranched or γ-branched amino acids at position *d* of a heptad repeat, while the reverse trend is true in tetrameric coiled coils.[32, 36]

It is well known that the incorporation of fluorinated side-chains into natural proteins and peptides can significantly modify their physico-chemical properties.[37-39] Substituting hydrophobic residues in the GCN4 leucine zipper for trifluoromethylleucine and/or trifluoromethylvaline can increase the thermal and chemical stability of the peptide dimer.[40] Peptides containing hexafluoroleucine can further oligomerize in membrane environments, forming discrete, bioorthogonal nanostructures.[41, 42] To explore the fluorous effect in β-peptide bundles, graduate student Matt Molski set out to replace the β^3L residues at positions 2 and 8 of Zwit-EYYK with hexafluoro-β^3-homoleucine (β^3L*, Figure 6b).[43] This exercise led to the peptides Zwit-2L* and Zwit-8L* (Figure 6a), which each contained a single fluorinated residue. While Zwit-8L* assembles into an octameric bundle analogous to the parental Zwit-EYYK, Zwit-2L* is tetrameric, similar to Zwit-VY. The association constants of Zwit-2L* and Zwit-8L* (ln K_a = 34 and 83, respectively) compare favorably with those of their non-fluorinated analogs, Zwit-VY and Zwit-EYYK (ln K_a = 38 and 94, respectively). Additionally, Zwit-8L* undergoes cold denaturation at concentrations where the octamer predominates (50 and 75 μM), a unique property that has not been previously observed in β-peptide

bundles. In a separate study, the Rosetta software package—which can now be applied to the design of β-peptides by including an extension for specifying initial bond lengths and angles in 14-helices—was used to generate a remodeled β-peptide bundle, Acid-1Y^{FF} (Figure 6a), containing phenylalanine side-chains in place of leucines at positions 5 and 8 of Acid-1Y. Incorporating a single pentafluoro-β^3-homophenylalanine (β^{3}F*, Figure 6b) residue to generate the analog Acid-1Y^{FF}* led to enhanced thermal stability (T_m = 67°C and 52°C at 200 μM Acid-1Y^{FF}* and Acid-1Y^{FF}, respectively), highlighting the stabilizing effect of fluorocarbon side-chains in these unnatural peptide oligomers.[44]

a)

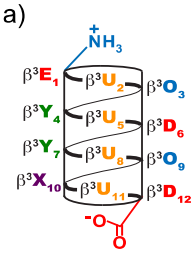

β^3-Peptide	U_2	U_5	U_8	U_{11}	X	*N*
Acid-VY	V	V	V	V	E	4
Zwit-VY	V	V	V	V	O	4
Acid-3Y	I	I	I	I	E	4
Zwit-2L*	L*	L	L	L	O	4
Zwit-8L*	L	L	L*	L	O	8
Acid-1Y^{FF}	L	F	F	L	E	8
Acid-1Y^{FF}*	L	F	F*	L	E	8

b)

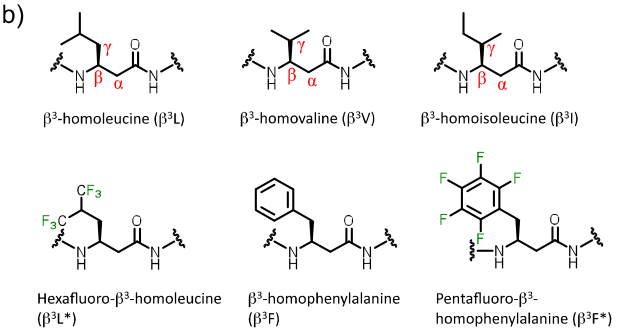

Figure 6. (a) Helical schematic of β-peptide bundles with alternate cores. *N* represents stoichiometry of self-assembly. (b) Side-chain chemical structures of residues in β-peptide bundle hydrophobic cores.

Overall, it is evident that the self-assembly properties of β-peptide bundles can be tuned by manipulating the side-chain composition within the hydrophobic core. In the Zwit-1F derived series of peptides, stoichiometry is controlled largely by the γ-carbon branching of hydrophobic residues; specifically, presence of γ-branching at all four core positions leads to tetramer formation, whereas the absence thereof results in octamer assembly. Another parameter that seemingly has an effect on β-peptide bundle stoichiometry is the monomer chain length – a computationally designed 14-helix consisting of 20 β^3-amino acid residues forms hexameric bundles despite having an all-β^{3}V face.[35] It is also possible to incorporate β-amino acids within longer α-amino acid peptides to assemble protein-like entities.[45-47] Further research to elucidate the relationship between β-peptide length, density, and oligomeric state would establish a more precise set of rules governing β-peptide bundle stoichiometry. These rules, together with the possibility of optimizing bundle stability by rational and computational design,[35, 44, 48-50] would help expand the repertoire of β-peptide-based artificial proteins and new catalysts with desirable properties.

From structure to activity: β-peptide bundles that fold and function

A ubiquitous feature of most complex biological systems is a sophisticated network of protein-protein and protein-small molecule interactions whose specificity relies on chemically and stereochemically defined active site or binding interfaces. Rational protein design is a process that uses a combination of structural information and predictive algorithms to generate novel proteins with desirable properties. By introducing mutations at strategic positions, a protein's binding or enzymatic activity can be improved, altered, or refined. Similar engineering principles can be applied to impart function to structurally characterized protein mimetics *via* the installation of appropriate chemical functionalities (Figure 7); the accessibility of most foldamers by solid phase synthesis also allows for the incorporation of a much more diverse set of side-chain chemistries. This section will describe the rational design of β-peptide bundles possessing carbohydrate recognition, metal binding, and catalytic activity.

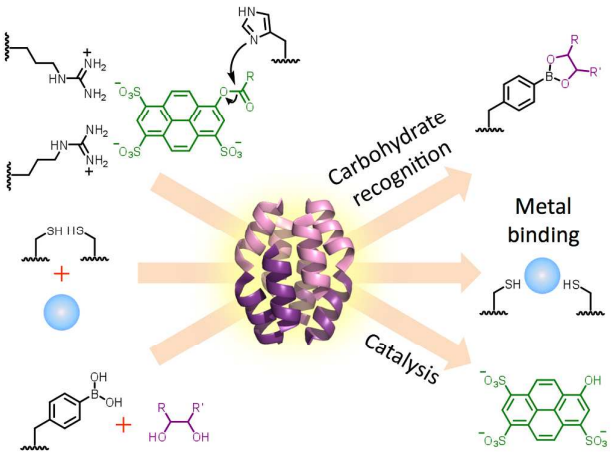

Figure 7. Functionalizing β-peptide bundles to impart carbohydrate recognition, metal binding, and catalytic activity.

Building a carbohydrate-sensing β-peptide bundle

Lectins are proteins found ubiquitously in nature that bind sugars through hydrogen bonding to hydroxyl groups and van der Waals interactions with the hydrocarbon skeleton. Synthetic lectins have many potential applications in medicine, nanotechnology, and analytical chemistry. Due to the relatively weak nature of protein-sugar interactions (often with association constants in the millimolar range), many synthetic carbohydrate sensors exploit boronic acids to coordinate diols and increase substrate affinity.[51-54] Boronic acids can also enhance the cytosolic delivery of polar macromolecules; in a recent report, boronated RNase A was internalized into mammalian cells through specific interactions with cell-surface glycans.[55]

Graduate student Michael Melicher was interested in the possibility that β-peptide bundles could be used as receptors to bind and differentiate sugars in aqueous solution–a challenging molecular recognition goal. Three boronic acid-containing β-peptide derivatives based on the stable octameric bundle Zwit-EYYK were designed. In each, one or both of the β^{3}Y residues on the aromatic

face of Zwit-EYYK were replaced by 4-borono-β^3-homophenylalanine (β^{3}B). One of these peptides, EYBK (Figure 8), retained the characteristic fold of Zwit-EYYK, assembling into an octamer with comparable thermodynamic properties (ln K_a = 85 and T_m = 83°C at 50 μM total peptide concentration). Using isothermal titration calorimetry (ITC), the association constants (K_a) of EYBK for catechol, dopamine, sorbitol, and mannitol in aqueous solution were determined to be 312, 814, 44, and 38 M^{-1}, respectively. Surprisingly, the affinities of these polyols for EYBK were all significantly lower than their affinities for phenylboronic acid (PBA), with catechol exhibiting a 25-fold difference between the two K_a values. Compared to a constitutively monomeric analog of EYBK, EYBK$_{ala}$, in which all core β^{3}L residues were replaced by β^3-homoalanine (β^{3}A), the octameric EYBK exhibited similar affinities for all four polyols, suggesting that polyols affinity did not benefit from bundle cooperatively. Interestingly, the affinity of the positively charged substrate dopamine for EYBK was 2-fold higher than for EYBK$_{ala}$, and only 4-fold lower than for PBA.[56]

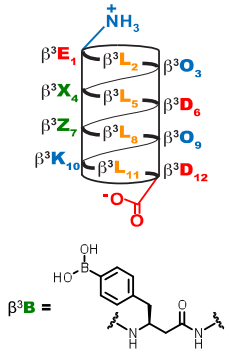

β^3-Peptide	X	Z	$K_{a,\ sorbitol}$ (M^{-1})
Zwit-EYYK	Y	Y	77.1 ± 7.5
EYBK	Y	B	43.8 ± 1.5
EOBK	O	B	4620 ± 212
EKBK	K	B	1040 ± 132
ERBK	R	B	1660 ± 124
EQBK	Q	B	758 ± 68.1
EOYK	O	Y	Not detected

Figure 8. Polyol binding β-peptide bundles, showing helical schematic (top left), chemical structure of 4-borono-β^3-homophenylalanine (bottom left), and the affinities of the EXBK analogs for sorbitol (right).

One hypothesis to account for the diminished affinity of EYBK for polyols other than dopamine focused on the electrostatic environment around the β^{3}B residue, which appeared to disfavor hydroxyl coordination. The high resolution X-ray structure of the EYBK bundle (Figure 9) revealed two unique boronic acid-containing sites: one at the interface of two parallel 14-helices (Type 1), and another at the interface where the two symmetry-related tetramer "hands" intersect (Type 2). Each EYBK octamer consists of four Type 1 and four Type 2 sites, with each Type 1 site spaced 12 Å away from the closest Type 2 site. The Type 1 and Type 2 sites differ in terms of both electrostatics and accessibility – Type 1 sites have greater negative potentials and larger solvent accessible surface areas than Type 2 sites. Nevertheless, both Type 1 and Type 2 boronic acids are surrounded by highly negative electrostatic environments that could inhibit carbohydrate binding.

To improve the affinity of EYBK for carbohydrate ligands, Melicher designed a series of new β-peptides, each containing a different residue at position 4, which is adjacent to the boronic acid at position 7 on the aromatic face (Figure 8). Replacing the original tyrosine side-chain with one containing a positive charge (ornithine, lysine, or arginine) would enable optimization of the electrostatic environment around the boronic acid without interfering with bundle self-assembly. As predicted, the calculated electrostatic potentials at both the Type 1 and Type 2 sites for the three EYBK analogs—EOBK, EKBK, and ERBK—were significantly more positive than those calculated for EYBK. Additionally, all three derivatives retained the ability to form octameric bundles as determined by SE-AU and CD experiments (ln K_a values between 55 and 75), consistent with the previous observation that β-peptide bundle quaternary structure is unaffected by changes to surface exposed residues.

In terms of carbohydrate binding, EOBK, EKBK, and ERBK all exhibited higher affinities for sorbitol relative to EYBK, with K_a = 4620, 1040, and 1660 M^{-1}, respectively, between 24- and 105-fold higher than the corresponding association constant for EYBK (K_a = 44 M^{-1}). Notably, an analog of EYBK containing β^3-homoglutamine (β^{3}Q) at position 4, EQBK, demonstrated weaker affinity for sorbitol (K_a = 758 M^{-1}) than the other EXBK analogs, suggesting that the cationically enhanced boronic acid sites favor polyol binding to a larger extent. Of the four EYBK-derived peptides, EOBK showed the greatest promise as a vehicle for complex sugar recognition.

The binding stoichiometry of the sorbitol•EOBK complex was determined to be 1:2 sorbitol:EOBK$_{monomer}$ using ITC, therefore, each EOBK octamer is complexed with 4 molecules of sorbitol. This observation most likely suggests that sorbitol binds preferentially to either the Type 1 or Type 2 boronic acids (4 of each type per bundle), rather than simultaneously to both. While the electrostatic potentials for the Type 1 and Type 2 sites in EOBK, EKBK, and ERBK are very similar, the Type 1 sites are generally twice as solvent accessible, highlighting the importance of sterics as well as electrostatics in β-peptide bundle carbohydrate recognition.

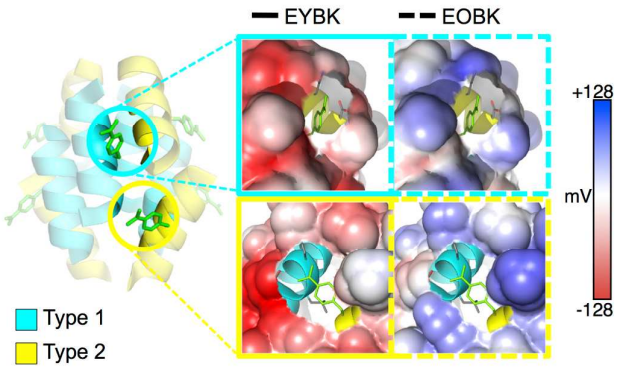

Figure 9. Structure of the EYBK bundle at 1.34 Å resolution (left) with 4-borono-β^3-homophenylalanine (β^{3}B) side-chains shown in green, and electrostatic surface potentials (right) calculated using Adaptive Poisson-Boltzmann Solver (APBS) of the Type 1 (cyan) and Type 2 (yellow) boronic acids in EYBK (solid boxes) and EOBK (dashed boxes). Unlike in previous figures, helices are colored here according to the type of boronic acid-containing site. Electrostatic potentials of both Type 1 and Type 2 sites in EYBK are negative, whereas those in EOBK are both positive – allowing the latter to bind carbohydrates more favorably.

In addition to the improved affinities of the EXBK bundles for sorbitol, EOBK and EKBK also bound the monosaccharide fructose reasonably (K_a = 663 and 364 M^{-1}, respectively). The parental EYBK bundle, by contrast, exhibited no detectable affinity for fructose, while PBA bound fructose with K_a <100 M^{-1}. Similarly, the β-peptide EOYK, which lacks a boronic acid side-chain and contains

a β^3Y residue in place of β^3B at position 7, did not form detectable complexes with either sorbitol or fructose, confirming that the boronic acids were indeed responsible for carbohydrate binding. Although none of the EYBK derivatives bound other simple saccharides tested (glucose, galactose, and sucrose), this innate specificity may be exploited for future designs of artificial β-peptide lectins. The improved affinities of the EXBK peptides for sorbitol and fructose represent a critical step towards the development of selective glycosyl transferases and hydrolases composed entirely of β^3-amino acids.[57] Recent results obtained in collaboration with the Miller lab, on the aqueous glycosylation of unprotected sucrose employing glycosyl fluorides in the presence of calcium ion and trimethylamine, in especially exciting in this regard.[58]

Allosteric metal ion binding β-peptide bundles

Nearly half of all characterized natural proteins require metals to carry out their biologic function. These metal ions can stabilize both ground state structure and transition state energies, thereby facilitating binding, transport, catalysis, and signal transduction.[59] Biological processes including photosynthesis, respiration, and nitrogen fixation all rely on metal ion cofactors; the magnesium-binding chlorophyll and iron-carrying hemoglobin are just two well-known examples of proteins whose structures embody metal ion centers. Proteins of known structure coordinate metal ions using imidazole, carboxylate, and thiolate side-chains belonging to histidine, glutamate/aspartate, and cysteine residues, although other amino acid side-chains as well as the peptide backbone have been shown to behave as dative ligands in certain cases.

Early work in the area of artificial metalloprotein design involved grafting heme centers, ranging from mono- to multi-heme maquettes, onto *de novo* α-helical bundles.[60] One designed di-heme-containing four-helix bundle binds oxygen with affinities and exchange timescales that match those of natural globins. This artificial oxygen transport protein consists of two bis-histidine metal coordination sites that exclude water, thereby reducing heme oxidation and stabilizing the oxygen-bound complex.[61] Similarly, the Cys_2His_2 motif has been engineered into helical bundles to successfully mimic zinc-finger proteins,[62] while a tris-Cys site has been incorporated into a synthetic three-stranded coiled coil, resembling the active site of the natural arsenic-binding protein ArsR.[63] Strategic replacement of residues with glutamate and histidine in self-associating peptides further led to the construction of heme-independent, dinuclear α-helical metallo-bundles capable of binding Zn(II), Co(II), or Fe(II).[64]

The prevalence of thiolate-rich metal coordination sites in nature, together with the precedence of cysteine-dependent artificial metalloproteins in the literature, inspired the design of a β-peptide bundle containing β^3-homocysteine (β^3C) residues for imparting metal ion binding activity.[65] Due to the unique nucleophilicity of cysteine thiols, placement of β^3C residues at positions other than the C-terminus leads to peptide self-cleavage via formation of a five-membered thiolactone (unpublished results). Therefore, in order to functionalize the thermodynamically stable bundle Zwit-EYYK for metal ion binding, β^3C was appended C-terminally as the thirteenth residue. The resultant peptide, Zwit-YK-C (Figure 10a), assembled into an octamer with ln K_a = 85, on par with the association constant of Zwit-EYYK (ln K_a = 94). A model of Zwit-YK-C based on the crystal structure of Zwit-EYYK reveals two types of stereochemically and electrostatically distinct metal binding sites, each containing two cysteinyl side-chains. The first type is formed at the termini of two parallel 14-helices, while the second type occurs at the tetramer-tetramer ("perpendicular") interface (Figure 10b and 10c). Each Zwit-YK-C octamer contains four Type 1 and two Type 2 sites, totalling 6 potential metal binding sites per bundle.

Zwit-YK-C was evaluated for binding to a panel of divalent cations, including Hg^{2+}, Pb^{2+}, Zn^{2+}, and Cd^{2+}. Metal coordination, however, was only detected in the presence of Cd^{2+}, which gave rise to a UV-vis spectroscopic signature characteristic of two-coordinate thiolate complexes, with an absorbance maximum occurring at <230 nm. Treatment of 100 μM Zwit-YK-C (95% bundle) with 0–75 μM Cd^{2+} led to a dose-dependent increase in the ligand-to-metal charge transfer (LMCT) signal intensity. Interestingly, a short, minimally structured control β-peptide (β-YACAACA) exhibits two different LMCT bands – one at 250 nm in the presence of 50 μM Cd^{2+}, and another at <230 nm in the presence of 200 μM Cd^{2+}. These UV-vis absorbance maxima are indicative of four- and two-coordinate thiolate binding, respectively. Given that β-YACAACA contains two β^3C residues and is likely unstructured in solution, this switch in metal coordination state is not surprising; at low Cd^{2+} concentrations, the thiol ligands are in excess, favoring higher coordination states, while the opposite is true at high Cd^{2+} concentrations. The lack of side-chain preorganization in β-YACAACA also means that the ligand binding geometry is relatively unrestricted, allowing for the formation of high-coordinate metal complexes. By contrast, four-coordinate binding is not observed for Zwit-YK-C even at very low Cd^{2+} concentrations, consistent with the modelled structure of Zwit-YK-C, in which only two-coordinate sites are present.

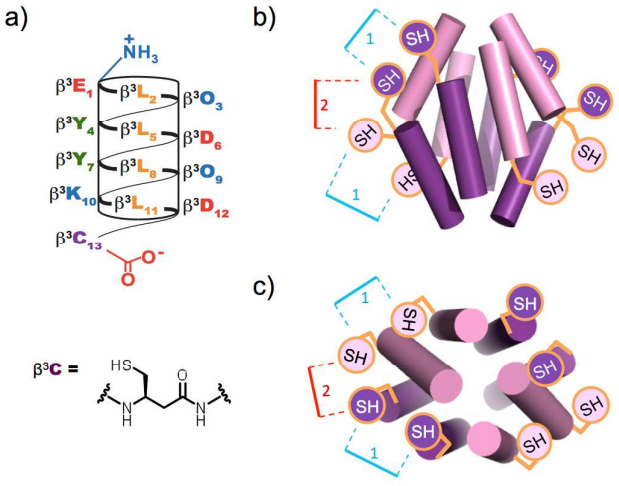

Figure 10. (a) Helical schematic of the 13-residue Zwit-YK-C, showing the chemical structure of the C-terminal β^3-homocysteine residue responsible for Cd^{2+} coordination. (b and c) Cartoon diagram of the Zwit-YK-C octamer model viewed from two different angles, illustrating the relative positions of the cysteinyl side-chains making up the Type 1 (blue) and Type 2 (red) metal binding sites.

Binding of Cd^{2+} ions also enhances the thermal stability of Zwit-YK-C, whose unfolding temperature T_m at 100 μM total peptide

concentration increases from 41.5°C in the absence of Cd^{2+} to >90°C upon addition of 30 μM Cd^{2+}. In addition, the stoichiometry of the metal-peptide complex, determined by reverse titration of Zwit-YK-C, is two Cd^{2+} ions per octamer. This 2:1 stoichiometry suggests that Cd^{2+} most likely occupies only the Type 2 sites, which are found exactly twice per bundle. A plot of absorbance at 245 nm as a function of Cd^{2+} concentration fits well to the Hill equation, returning a Hill coefficient $n_h = 1.9$, which implies that the two metal ions bind Zwit-YK-C cooperatively. The apparent K_d calculated from this fit is in reasonable agreement with that determined using ITC (15.3 μM and 39 μM, respectively). Although the metal ion affinity of Zwit-YK-C is roughly two orders of magnitude lower than that of a designed three-helix α-peptide bundle, α_3DIV, the binding constants are not directly comparable due to differences in coordination geometry.[66]

While the origin of positive cooperativity in β-peptide metal coordination remains unclear, this behavior is reminiscent of substrate binding in natural proteins. The preference of Zwit-YK-C for Cd^{2+} over other metal ions further highlights the innate selectivity of β-peptide bundles, which can be exploited for future designs of metal-binding proteomimetic materials with sophisticated function.

Design of a β-peptide bundle catalyst

Peptides embody two fundamental properties that engender chemical catalysis. The propensity of a polyamide backbone to occupy a restricted conformational space simplifies the placement of potential catalytic groups, while the chirality of amino acid monomers and the structures they form favors selective reactivity.[67-69] Over the past few decades, polyamides composed of both natural and non-natural α-peptides have been reported to affect the rate, regioselectivity and stereoselectivity of a diverse set of organic transformations. Despite the extensive literature on catalytic α-peptides, there have been surprisingly few reports of peptidic organocatalysts that contain backbone-modified amino acid building blocks. These examples include a β-peptide that assembles into a mixture of oligomeric states and promotes a retroaldol reaction,[70] a short α/β-peptide that catalyzes intra- and intermolecular aldol reactions,[71] a poly-β-leucine catalyst for the Juliá-Colonna asymmetric epoxidation of enones,[72] and an α/β/γ-peptide chimera that facilitates a native chemical ligation reaction.[73] Although in all four cases the specified reaction rate was increased by the presence of the catalyst, none of the studies fully exploited the ability of synthetic peptides to adopt higher-order structures. In this realm, the series of self-assembling β-peptide bundles developed by our research group provides an excellent starting point for the discovery of novel peptidomimetic catalysts with higher-order, protein-like folds.

Ester hydrolysis is one of the most well characterized reactions in water. Peptide-based ester hydrolases were identified as early as the 1980s; in initial studies, short dipeptides and tripeptides embedded in surfactants were shown to be capable of deacylating long *p*-nitrophenyl (PNP) esters with enantioselectivity (achieving at best $k_{cat}^{L}/k_{cat}^{D} = 83.6$).[74-76] Linear and cyclic peptides containing histidine, serine, and aspartic acid residues were later demonstrated to possess enantioselective hydrolase activity on various PNP esters in the absence of a surfactant.[77-79] Larger peptides with protein-like architectures have also been explored in the development of artificial esterases. Baltzer's *de novo* designed helix-loop-helix polypeptides accelerated the hydrolysis rate of PNP esters by a substantial 1140-fold relative to the 4-methylimidazole-catalyzed reaction.[80] More recently, dendritic peptides identified by a combinatorial screen led to significant enhancements in the rate of ester hydrolysis (up to $k_{cat}/k_{uncat} = 2000$ at neutral pH) under various conditions.[81] Notably, these dendrimers have a broader substrate scope, ranging from negatively charged pyrenesulfonate esters to positively charged quinolinium esters.[82] One explanation for the high efficiency and relative promiscuity of dendritic catalysts is that as high-molecular weight (almost 5000 Da) globular macromolecules, they likely comprise distinct active sites, each preferentially binding one type of substrate. β-peptide bundles, when assembled, are also globular and range from roughly 8–15 kDa in size, which should confer a similar advantage on their molecular recognition properties.

The robust octamer Zwit-EYYK was again used as a scaffold for the design of a β-peptide capable of catalyzing a model reaction—hydrolysis of 8-acetoxypyrene-1,3,6-trisulfonate (**1**)—which releases the fluorescent product pyranine (**2**) upon cleavage of the ester bond (Scheme 1).

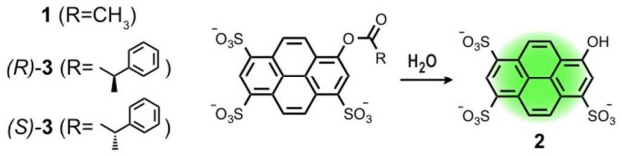

Scheme 1. Hydrolysis of pyrene trisulfonate esters, the model reaction used in the study of β-peptide bundle esterases.

To increase the affinity of Zwit-EYYK for the negatively charged substrate **1**, the β^3O residues at positions 3 and 9 were replaced with β^3-homoarginine (β^3R, Figure 11a). Given the highly similar electrostatic properties of β^3O and β^3R, this modification was not expected to significantly disrupt the β-peptide bundle quaternary structure. A catalytic histidine residue (αH, Figure 11a) was also installed at position 1 (β^3E in Zwit-EYYK) to avoid disruption of the 14-helix backbone as a result of introducing an internal α-amino acid. In the presence of this modified peptide, βEst-2 (Figure 11b), hydrolysis of **1** fit best to a Michaelis-Menten model, returning the kinetic parameters $k_{cat} = 0.018$ min^{-1} and $K_M = 345$ μM, and a specificity constant $k_{cat}/K_M = 54$ M^{-1}min^{-1}. Relative to the uncatalyzed reaction, βEst-2 enhanced the rate of hydrolysis of **1** by a k_{cat}/k_{uncat} ratio of 588. Overall, these kinetic constants are comparable with those of a similarly sized dendritic catalyst of the same reaction ($k_{cat}/K_M = 120$ M^{-1}min^{-1}; $k_{cat}/k_{uncat} = 340$).[81] Zwit-EYYK, as expected, exhibited no detectable levels of esterolytic activity.

While βEst-2 was 14-helical by CD spectroscopy and retained the ability to self-assemble into bundles at high concentration (400 μM), it was primarily monomeric at the concentration chosen for the steady-state kinetics studies (25 μM). Examination of the Zwit-EYYK X-ray structure reveals that the β^3E at position 1 is involved in an interhelical salt-bridge interaction; substituting this residue for αH may have a destabilizing effect on the βEst-2 quaternary structure. To recover bundle stability, several designs were pursued, two of which significantly improved oligomer formation at 25 μM

concentration. The first strategy involved restoring β^3E_1 and appending the catalytic αH residue to the C-terminus, similar to the design of Zwit-YK-C, while the second strategy aimed to harness entropic effects by covalently joining two βEst-2 monomers via a 4×βG linker in a manner analogous to the design of Z28.[31] Both of these peptides, βEst-2C (Figure 11c) and βEst-28 (Figure 11d), exhibited significantly higher degrees of self-assembly (>80% bundle at 25 μM) compared to βEst-2.

In terms of activity, βEst-2C is roughly twice as efficient as βEst-2 at catalyzing the hydrolysis of **1**, achieving k_{cat}/K_M = 98 $M^{-1}min^{-1}$ and k_{cat}/k_{uncat} = 460 under the same conditions. Intriguingly, a related peptide, βEst-2N, which contains a N-terminal αH residue, was virtually inactive at 25 μM (k_{cat}/K_M = 3 $M^{-1}min^{-1}$) despite having a similar degree of association as βEst-2C. Assuming that βEst-2N and βEst-2C adopt the same octameric architecture as Zwit-EYYK, this drastic difference in catalytic activity can be rationalized as follows: Attaching the αH to the N-terminus in the case of βEst-2N places the catalytic side-chain on the same face as the β^3R residues involved in binding, creating a sub-optimal active site geometry. On the other hand, appending the αH to the C-terminus as in βEst-2C presents the catalytic and binding residues on separate faces, favoring catalysis. The dependence of catalytic function on the geometric arrangement of the αH and β^3R residues suggests that peptide-substrate interactions are highly specific, and point to the existence of well-defined active sites.

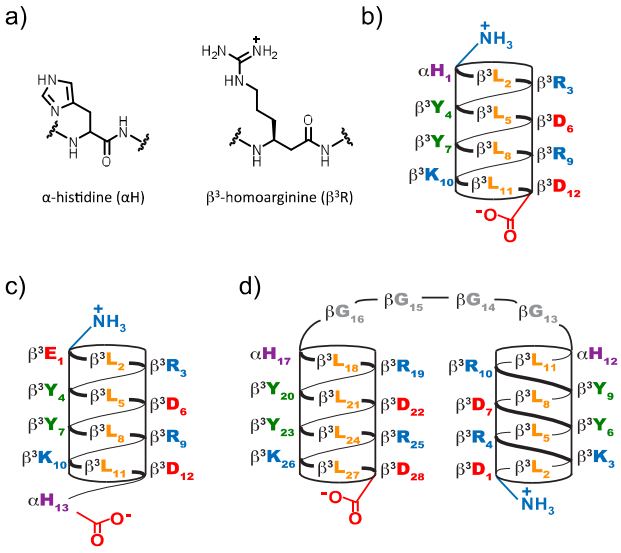

Figure 11. (a) Chemical structures of the residues incorporated into Zwit-EYYK analogs to impart catalytic function. (b-d) Helical schematics of (b) βEst-2, (c) βEst-2C, and (d) βEst-28.

While the relative positions of the αH and β^3R residues in βEst-28 mimic those in βEst-2, βEst-28 exhibited an unexpected kinetic profile that disobeyed the Michaelis-Menten model of catalysis. Rather than undergoing the typical hyperbolic increase as a function of substrate concentration, the hydrolysis rate of **1** in the presence of βEst-28 reached a maximum at [**1**] = 200 μM, then steadily descended towards an asymptote at higher substrate concentrations. This behavior is indicative of substrate inhibition, a well-characterized phenomenon that occurs in an estimated 20% of natural enzymes as a regulatory mechanism. Enzymes such as tyrosine hydroxylase, acetylcholinesterase, and DNA methyltransferases are all inhibited at saturating concentrations of their respective substrates to avoid excessive production or degradation of molecules important in metabolic pathways.[83, 84] Fitting the hydrolysis kinetics of **1** in the presence of βEst-28 to the Haldane equation,[85] which accounts for substrate inhibition through the inclusion of an additional equilibrium constant K_i, returned a k_{cat}/K_M value of 5102 $M^{-1}min^{-1}$, nearly two orders of magnitude greater than that for βEst-2. The steady-state kinetic constants for βEst-28 (k_{cat} = 0.020 min^{-1}; K_M = 4 μM) agreed reasonably with analogous parameters obtained from pre-steady-state studies (k_{chem} = 0.083 min^{-1}; $K_{d,\ apparent}$ = 14 μM), providing support for the substrate inhibition model.

The improved catalytic efficiencies of βEst-2C and βEst-28 relative to βEst-2 result directly from greatly increased substrate affinities (K_M = 4, 147, and 345 μM for βEst-28, βEst-2C and βEst-2, respectively), highlighting the benefit of a catalyst possessing the β-peptide bundle quaternary fold. A comparison between βEst-2C and its stoichiometric derivatives—βEst-2C-V and βEst-2C-A, in which the core β^3L residues were substituted for β^3V or β^3A, respectively—reveals that bundle formation indeed plays a critical role in catalysis. While the octameric βEst-2C and the tetrameric βEst-2C-V exhibited similar specificity constants (k_{cat}/K_M = 98 and 73 $M^{-1}min^{-1}$), βEst-2C-A, a constitutive monomer, was minimally active (k_{cat}/K_M = 8 $M^{-1}min^{-1}$). The high resolution X-ray structure of βEst-2C further suggests the presence of 20 potential interhelical active sites per octameric bundle – 8 at the parallel, 4 at the antiparallel, and 8 at the tetramer-tetramer interface. This abundance of active sites is sufficient to explain the difference in catalytic efficiency between βEst-2C, βEst-2C-V, and βEst-2C-A, even if occupancy is low.

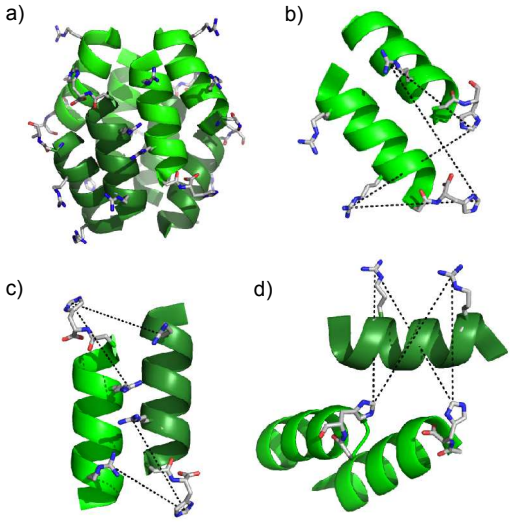

Figure 12. (a) Structure of the βEst-2C octamer at 1.81 Å resolution, showing the arginyl and histidyl side-chains in gray. Shading corresponds to helix orientation. (b-d) Putative active sites at the (b) parallel, (c) antiparallel, and (d) tetramer-tetramer helical interfaces.

The complex three-dimensional chemical environment on the surface of βEst-2C confers an additional advantage on its catalytic properties – enantioselectivity. Between the enantiomeric substrates (*R*)-**3** and (*S*)-**3** (Scheme 1), βEst-2C accelerates the hydrolysis of (*R*)-**3** four times as much as it does that of (*S*)-**3**.[86] This chiral selectivity is comparable with that of a dendritic esterase, which favors the hydrolysis of (*S*)-**3** with an enantiomeric ratio $E = 2.8$.[82]

Overall, the series of β-peptide bundle esterases described here represent an important step towards the development of oligomeric catalysts containing β^3-amino acids. The structurally complex octameric fold not only allows for the formation of well-defined active sites that are electrostatically and stereochemically unique, but also provides a thermodynamically stable scaffold that is amenable to functionalization.

Conclusions and outlook

Polymers and oligomers formed from β^3-amino acids possess two properties that have attracted attention from a broad coalition of physical and biomedical scientists. The first property, and the foundation for the discoveries described in this Perspective, is the demonstrated ability to fold in water solvent into stable, protein-like, tertiary and quaternary structures. Although this Perspective focuses on the quaternary structures known as β-peptide bundles, we note that β^3-amino acids have also been incorporated into structurally well-defined bundles that contain both α- and β-amino acids,[45-47] cyclic nanotubes,[19] and supramolecular foldamer architectures (foldectures) that possess tunable dimensions and shapes[87-92] and magnetotactic behavior.[93] Much current research, in our lab and elsewhere, seeks to exploit these higher-order structures to encode ever more sophisticated function.

The second property embodied by β-amino acid oligomers is their documented ability to evade two cellular processes that currently limit the effectiveness of α-peptides and proteins as research tools (if not more): proteases and the adaptive immune response. Indeed, it has been more than 20 years since Seebach reported that certain β-peptides could resist the catalytic action of the protease pepsin;[94] subsequent studies have confirmed that β-peptides are resistant to most, if not all, mammalian proteases.[95-99] More recent, important work from Gellman and others has detailed the effects of β-amino acid substitutions on binding to MHC molecules and/or recognition by T-cell receptors.[100-103] In this case, it is clear that multiple β-amino acid substitutions may be necessary to avoid MHC engagement.

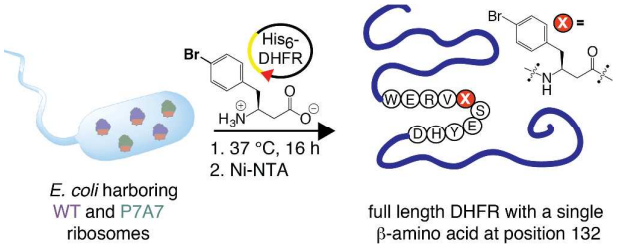

Figure 13. *In vivo* biosynthesis of a β-amino acid-containing protein.[104]

But despite the unique and important attributes of β-amino acids, their potential for biotechnology applications remains underexploited, in large part because until very recently, β-peptides could only be synthesized using chemical methods and screened for activity. Indeed, the concept of synthesizing a β-peptide on the ribosome–let alone in engineered bacterial strains compatible with molecular evolution methods–seemed unconditionally out of reach. Excitingly, in 2013 Sidney Hecht and his coworkers reported that mutant ribosomes in S30 cell extracts from certain erythromycin-resistant *E. coli* mutants could incorporate a small number of β-amino acids into a full length protein *in vitro*.[105-107] More recently, Murakami and coworkers exploited an optimized bacterial cell-free translation system containing wild type ribosomes and excess elongation factor Tu (EF-Tu) to synthesize peptides containing multiple β-amino acids.[108] Building on these important discoveries, and buoyed by early work of Szostak,[109] our group reported that β^3-amino acids are adequate substrates for several wild type *E. coli* aminoacyl-tRNA synthetases, and that one enzyme, phenylalanyl-tRNA synthetase (PheRS), can collaborate with wild type EF-Tu and ribosomes containing mutant peptidyl transferase centers to incorporate β^3-homophenylalanine derivatives into full length DHFR *in vivo*.[104] *E. coli* harboring the most active mutant ribosome P7A7 are robust, with a doubling time only 14% longer than wild type. These results emphasize the unexpected tolerance of *E. coli* and its translation machinery to the β-amino acid backbone and set the stage for *in vivo* selections to evolve orthogonal translational machinery components for the site-selective incorporation of diverse β-amino acids into proteins and polypeptides. *E. coli* harboring mutant ribosomes may possess the capacity to incorporate many non-natural, non-α-amino acids into proteins and other sequence-programmed polymeric materials with wide-ranging utility. Ultimately, a ribosome tailored to process β-amino acid substrates would open up endless opportunities for exploring the structure and function of *bona fide* "β-proteins".

Acknowledgements

The authors are grateful to all members of the Schepartz group, past and present, for establishing an environment of collaboration and creativity that supports even highly unexpected discoveries.

Notes and references

1. T. Svedberg and R. Fahraeus, *J Am Chem Soc*, 1926, **48**, 430-438.
2. I. M. Klotz, N. R. Langerman and D. W. Darnall, *Ann Rev Biochem*, 1970, **39**, 25-62.
3. J. W. Bryson, S. F. Betz, H. S. Lu, D. J. Suich, H. X. X. Zhou, K. T. Oneil and W. F. Degrado, *Science*, 1995, **270**, 935-941.
4. C. A. Mirkin, R. L. Letsinger, R. C. Mucic and J. J. Storhoff, *Nature*, 1996, **382**, 607-609.
5. J. D. Hartgerink, T. D. Clark and R. M. Ghadiri, *Chem Eur J*, 1998, **4**, 1367 - 1372.
6. A. Shimojima, Z. Liu, T. Ohsuna, O. Terasaki and K. Kuroda, *J Am Chem Soc*, 2005, **127**, 14108-14116.

7. C. M. Goodman, S. Choi, S. Shandler and W. F. DeGrado, *Nat Chem Biol*, 2007, **3**, 252-262.
8. A. D. Bautista, C. J. Craig, E. A. Harker and A. Schepartz, *Curr Op Chem Biol*, 2007, **11**, 685-692.
9. S. H. Gellman, *Accts Chem Red*, 1998, **31**, 173-180.
10. D. Seebach and J. Gardiner, *Accts Chem Red*, 2008, **41**, 1366-1375.
11. D. Seebach, D. F. Hook and A. Glattli, *Biopolymers*, 2006, **84**, 23-37.
12. C. Baldauf, R. Gunther and H. J. Hofmann, *J Org Chem*, 2004, **69**, 6214-6220.
13. R. J. Simon, R. S. Kania, R. N. Zuckermann, V. D. Huebner, D. A. Jewell, S. Banville, S. Ng, L. Wang, S. Rosenberg, C. K. Marlowe, D. C. Spellmeyer, R. Y. Tan, A. D. Frankel, D. V. Santi, F. E. Cohen and P. A. Bartlett, *Proc Natl Acad Sci USA*, 1992, **89**, 9367-9371.
14. A. Zega, *Curr Med Chem*, 2005, **12**, 589-597.
15. G. W. Collie, K. Pulka-Ziach, C. M. Lombardo, J. Fremaux, F. Rosu, M. Decossas, L. Mauran, O. Lambert, V. Gabelica, C. D. Mackereth and G. Guichard, *Nature Chemistry*, 2015, **7**, 871-878.
16. D. Seebach, A. K. Beck and D. J. Bierbaum, *Chem Biodivers*, 2004, **1**, 1111-1239.
17. D. S. Daniels, E. J. Petersson, J. X. Qiu and A. Schepartz, *J Am Chem Soc*, 2007, **129**, 1532-1533.
18. E. J. Petersson, C. J. Craig, D. S. Daniels, J. X. Qiu and A. Schepartz, *J Am Chem Soc*, 2007, **129**, 5344-5345.
19. T. D. Clark, L. K. Buehler and M. R. Ghadiri, *J Am Chem Soc*, 1998, **120**, 651-656.
20. T. L. Raguse, J. R. Lai, P. R. LePlae and S. H. Gellman, *Org Lett*, 2001, **3**, 3963-3966.
21. H. Wendt, C. Berger, A. Baici, R. M. Thomas and H. R. Bosshard, *Biochemistry*, 1995, **34**, 4097-4107.
22. H. Wendt, L. Leder, H. Harma, I. Jelesarov, A. Baici and H. R. Bosshard, *Biochemistry*, 1997, **36**, 204-213.
23. X. M. Yang, W. F. Yu, J. H. Li, J. Fuchs, J. Rizo and M. L. Tasayco, *J Am Chem Soc*, 1998, **120**, 7985-7986.
24. R. P. Cheng and W. F. DeGrado, *J Am Chem Soc*, 2002, **124**, 11564-11565.
25. E. K. O'Shea, K. J. Lumb and P. S. Kim, *Curr Biol*, 1993, **3**, 658-667.
26. S. A. Hart, A. B. F. Bahadoor, E. E. Matthews, X. Y. J. Qiu and A. Schepartz, *J Am Chem Soc*, 2003, **125**, 4022-4023.
27. J. A. Kritzer, J. Tirado-Rives, S. A. Hart, J. D. Lear, W. L. Jorgensen and A. Schepartz, *J Am Chem Soc*, 2005, **127**, 167-178.
28. J. X. Qiu, E. J. Petersson, E. E. Matthews and A. Schepartz, *J Am Chem Soc*, 2006, **128**, 11338-11339.
29. J. L. Goodman, E. J. Petersson, D. S. Daniels, J. X. Qiu and A. Schepartz, *J Am Chem Soc*, 2007, **129**, 14746-14751.
30. C. J. Craig, J. L. Goodman and A. Schepartz, *ChemBiochem*, 2011, **12**, 1035-1038.
31. E. J. Petersson and A. Schepartz, *J Am Chem Soc*, 2008, **130**, 821-823.
32. P. B. Harbury, T. Zhang, P. S. Kim and T. Alber, *Science*, 1993, **262**, 1401-1407.
33. J. L. Goodman, M. A. Molski, J. Qiu and A. Schepartz, *ChemBiochem*, 2008, **9**, 1576-1578.
34. P. S.-P. Wang, C. J. Craig and A. Schepartz, *Tetrahedron*, 2012, **68**, 4342-4345.
35. I. V. Korendovych, Y. H. Kim, A. H. Ryan, J. D. Lear, W. F. DeGrado and S. J. Shandler, *Org Lett*, 2010, **12**, 5142-5145.
36. A. N. Lupas and M. Gruber, *Adv Protein Chem*, 2005, **70**, 37-78.
37. K. H. Lee, H. Y. Lee, M. M. Slutsky, J. T. Anderson and E. N. G. Marsh, *Biochemistry*, 2004, **43**, 16277-16284.
38. E. N. G. Marsh, *Chem Biol*, 2000, **7**, R153-R157.
39. B. C. Buer, J. L. Meagher, J. A. Stuckey and E. N. G. Marsh, *Proc Natl Acad Sci USA*, 2012, **109**, 4810-4815.
40. B. Bilgicer, A. Fichera and K. Kumar, *J Am Chem Soc*, 2001, **123**, 4393-4399.
41. L. M. Gottler, R. D. Bea, C. E. Shelburne, A. Ramamoorthy and E. N. G. Marsh, *Biochemistry*, 2008, **47**, 9243-9250.
42. M. Cametti, B. Crousse, P. Metrangolo, R. Milani and G. Resnati, *Chem Soc Rev*, 2012, **41**, 31-42.
43. M. A. Molski, J. L. Goodman, C. J. Craig, H. Meng, K. Kumar and A. Schepartz, *J Am Chem Soc*, 2010, **132**, 3658-3659.
44. M. A. Molski, J. L. Goodman, F.-C. Chou, D. Baker, R. Das and A. Schepartz, *Chem Sci*, 2013, **4**, 319-324.
45. W. S. Horne, J. L. Price, J. L. Keck and S. H. Gellman, *J Am Chem Soc*, 2007, **129**, 4178-+.
46. M. W. Giuliano, W. S. Horne and S. H. Gellman, *J Am Chem Soc*, 2009, **131**, 9860-+.
47. J. L. Price, W. S. Horne and S. H. Gellman, *J Am Chem Soc*, 2010, **132**, 12378-12387.
48. K. Drew, P. D. Renfrew, T. W. Craven, G. L. Butterfoss, F.-C. Chou, S. Lyskov, B. N. Bullock, A. Watkins, J. W. Labonte, M. Pacella, K. P. Kilambi, A. Leaver-Fay, B. Kuhlman, J. J. Gray, P. Bradley, K. Kirshenbaum, P. S. Arora, R. Das and R. Bonneau, *Plos One*, 2013, **8**.
49. S. J. Shandler, M. V. Shapovalov, R. L. Dunbrack and W. F. DeGrado, *J Am Chem Soc*, 2010, **132**, 7312-7320.
50. S. J. Shandler, I. V. Korendovych, D. T. Moore, K. B. Smith-Dupont, C. N. Streu, R. I. Litvinov, P. C. Billings, F. Gai, J. S. Bennett and W. F. DeGrado, *J Am Chem Soc*, 2011, **133**, 12378-12381.
51. M. Mazik, *Chem Soc Rev*, 2009, **38**, 935-956.
52. T. D. James and S. Shinkai, *Top Curr Chem*, 2002, **218**, 159-200.
53. T. D. James, K. R. A. S. Sandanayake and S. Shinkai, *Angew Chem Int Ed*, 1996, **35**, 1910-1922.
54. S. Striegler, *Curr Org Chem*, 2003, **7**, 81-102.
55. G. A. Ellis, M. J. Palte and R. T. Raines, *J Am Chem Soc*, 2012, **134**, 3631-3634.
56. M. S. Melicher, J. Chu, A. S. Walker, S. J. Miller, R. H. G. Baxter and A. Schepartz, *Org Lett*, 2013, **15**, 5048-5051.
57. M. S. Melicher, A. S. Walker, J. Shen, S. J. Miller and A. Schepartz, *Org Lett*, 2015, **17**, 4718-4721.
58. G. Pelletier, A. Zwicker, C. L. Allen, A. Schepartz and S. J. Miller, *J Am Chem Soc*, 2016, DOI: 10.1021/jacs.5b13384.
59. Y. Lu, N. Yeung, N. Sieracki and N. M. Marshall, *Nature*, 2009, **460**, 855-862.
60. R. B. Hill, D. P. Raleigh, A. Lombardi and W. F. Degrado, *Accts Chem Red*, 2000, **33**, 745-754.
61. E. A. Berry and F. A. Walker, *J Biol Inorg Chem*, 2008, **13**, 481-498.
62. M. Klemba and L. Regan, *Biochemistry*, 1995, **34**, 10094-10100.
63. D. S. Touw, C. E. Nordman, J. A. Stuckey and V. L. Pecoraro, *Proc Natl Acad Sci USA*, 2007, **104**, 11969-11974.

64. A. Lombardi, C. M. Summa, S. Geremia, L. Randaccio, V. Pavone and W. F. DeGrado, *Proc Natl Acad Sci USA*, 2000, **97**, 6298-6305.
65. J. P. Miller, M. S. Melicher and A. Schepartz, *J Am Chem Soc*, 2014, **136**, 14726-14729.
66. S. Chakraborty, J. Y. Kravitz, P. W. Thulstrup, L. Hemmingsen, W. F. DeGrado and V. L. Pecoraro, *Angew Chem Int Ed*, 2011, **50**, 2049-2053.
67. E. N. Jacobsen and D. W. C. MacMillan, *Proc Natl Acad Sci USA*, 2010, **107**, 20618-20619.
68. R. R. Knowles and E. N. Jacobsen, *Proc Natl Acad Sci USA*, 2010, **107**, 20678-20685.
69. E. A. C. Davie, S. M. Mennen, Y. Xu and S. J. Miller, *Chem Rev*, 2007, **107**, 5759-5812.
70. M. M. Muller, M. A. Windsor, W. C. Pomerantz, S. H. Gellman and D. Hilvert, *Angew Chem Int Ed*, 2009, **48**, 922-925.
71. V. D'elia, H. Zwicknagl and O. Reiser, *J Org Chem*, 2008, **73**, 3262-3265.
72. P. E. Coffey, K. H. Drauz, S. M. Roberts, J. Skidmore and J. A. Smith, *Chemical Communications*, 2001, DOI: Doi 10.1039/B106368p, 2330-2331.
73. R. R. Araghi and B. Koksch, *Chemical Communications*, 2011, **47**, 3544-3546.
74. K. Ohkubo and N. Matsumoto, *J Mol Catal*, 1982, **17**, 23-27.
75. K. Ohkubo, N. Matsumoto and H. Ohta, *J Chem Soc Chem Comm*, 1982, DOI: Doi 10.1039/C39820000738, 738-740.
76. K. Ohkubo, K. Sugahara, K. Yoshinaga and R. Ueoka, *J Chem Soc Chem Comm*, 1980, DOI: Doi 10.1039/C39800000637, 637-639.
77. M. Kodaka, *B Chem Soc Jpn*, 1983, **56**, 3857-3858.
78. N. Nishi, B. Nakajima, M. Morishige and S. Tokura, *Int J Pept Prot Res*, 1986, **27**, 261-268.
79. R. Ueoka, Y. Matsumoto and Y. Ihara, *Chemistry Letters*, 1984, DOI: Doi 10.1246/Cl.1984.1807, 1807-1810.
80. K. S. Broo, H. Nilsson, J. Nilsson and L. Baltzer, *J Am Chem Soc*, 1998, **120**, 10287-10295.
81. S. Javor, E. Delort, T. Darbre and J. L. Reymond, *J Am Chem Soc*, 2007, **129**, 13238-13246.
82. C. Douat-Casassus, T. Darbre and J. L. Reymond, *J Am Chem Soc*, 2004, **126**, 7817-7826.
83. N. S. Quinsey, A. Q. Luong and P. W. Dickson, *J Neurochem*, 1998, **71**, 2132-2138.
84. M. C. Reed, A. Lieb and H. F. Nijhout, *Bioessays*, 2010, **32**, 422-429.
85. J. B. S. Haldane, *Enzymes*, Longmans, Green and Co., New York, 1930.
86. P. S. P. Wang, J. B. Nguyen and A. Schepartz, *J Am Chem Soc*, 2014, **136**, 6810-6813.
87. S. Kwon, A. Jeon, S. H. Yoo, I. S. Chung and H. S. Lee, *Angew Chem Int Ed*, 2010, **49**, 8232-8236.
88. J. Kim, S. Kwon, S. H. Kim, C. K. Lee, J. H. Lee, S. J. Cho, H. S. Lee and H. Ihee, *J Am Chem Soc*, 2012, **134**, 20573-20576.
89. S. H. Yoo, T. Eom, S. Kwon, J. Gong, J. Kim, S. J. Cho, R. W. Driver, Y. Lee, H. Kim and H. S. Lee, *J Am Chem Soc*, 2015, **137**, 2159-2162.
90. S. Kwon, H. S. Shin, J. Gong, J. H. Eom, A. Jeon, S. H. Yoo, I. S. Chung, S. J. Cho and H. S. Lee, *J Am Chem Soc*, 2011, **133**, 17618-17621.
91. J. H. Eom, J. Gong, R. Jeong, R. W. Driver and H. S. Lee, *Solid State Sci*, 2015, **48**, 39-43.
92. J. H. Eom, J. Gong, S. Kwon, A. Jeon, R. Jeong, R. W. Driver and H. S. Lee, *Angew Chem Int Ed*, 2015, **54**, 13204-13207.
93. S. Kwon, B. J. Kim, H. K. Lim, K. Kang, S. H. Yoo, J. Gong, E. Yoon, J. Lee, I. S. Choi, H. Kim and H. S. Lee, *Nat Commun*, 2015, **6**.
94. D. Seebach, M. Overhand, F. N. M. Kuhnle, B. Martinoni, L. Oberer, U. Hommel and H. Widmer, *Helv Chim Acta*, 1996, **79**, 913-941.
95. B. Geueke, T. Heck, M. Limbach, V. Nesatyy, D. Seebach and H. P. E. Kohler, *FEBS J*, 2006, **273**, 5261-5272.
96. B. Geueke and H. P. E. Kohler, *Appl Micro Biotech*, 2007, **74**, 1197-1204.
97. H. N. Gopi, G. Ravindra, P. P. Pal, P. Pattanaik, H. Balaram and P. Balaram, *FEBS Lett*, 2003, **535**, 175-178.
98. T. Heck, M. Limbach, B. Geueke, M. Zacharias, J. Gardiner, H. P. E. Kohler and D. Seebach, *Chem Biodiv*, 2006, **3**, 1325-1348.
99. D. F. Hook, P. Bindschadler, Y. R. Mahajan, R. Sebesta, P. Kast and D. Seebach, *Chem Biodiv*, 2005, **2**, 591-632.
100. G. Guichard, A. Zerbib, F. A. Le Gal, J. Hoebeke, F. Connan, J. Choppin, J. P. Briand and J. G. Guillet, *J Med Chem*, 2000, **43**, 3803-3808.
101. S. Reinelt, M. Marti, S. Dedier, T. Reitinger, G. Folkers, J. A. L. de Castro and D. Rognan, *J Biol Chem*, 2001, **276**, 24525-24530.
102. A. I. Webb, M. A. Dunstone, N. A. Williamson, J. D. Price, A. de Kauwe, W. S. Chen, A. Oakley, P. Perlmutter, J. McCluskey, M. I. Aguilar, J. Rossjohn and A. W. Purcell, *J Immunol*, 2005, **175**, 3810-3818.
103. R. W. Cheloha, J. A. Sullivan, T. Wang, J. M. Sand, J. Sidney, A. Sette, M. E. Cook, M. Suresh and S. H. Gellman, *ACS Chem Bio*, 2015, **10**, 844-854.
104. C. M. Czekster, W. E. Robertson, A. S. Walker, D. Söll and A. Schepartz, *J Am Chem Soc*, 2016, **138**, in press.
105. L. M. Dedkova, N. E. Fahmi, R. Paul, M. del Rosario, L. Zhang, S. Chen, G. Feder and S. M. Hecht, *Biochemistry*, 2012, **51**, 401-415.
106. R. Maini, S. R. Chowdhury, L. M. Dedkova, B. Roy, S. M. Daskalova, R. Paul, S. Chen and S. M. Hecht, *Biochemistry*, 2015, DOI: 10.1021/acs.biochem.5b00389.
107. R. Maini, D. T. Nguyen, S. Chen, L. M. Dedkova, S. R. Chowdhury, R. Alcala-Torano and S. M. Hecht, *Bioorg Med Chem*, 2013, **21**, 1088-1096.
108. T. Fujino, Y. Goto, H. Suga and H. Murakami, *J Am Chem Soc*, 2016, **138**.
109. M. C. T. Hartman, K. Josephson and J. W. Szostak, *Proc Natl Acad Sci USA*, 2006, **103**, 4356-4361.

